Journal of the Korean Institute of Illuminating and Electrical Installation Engineers Vol. 17, No.1, pp. 80~85 January 2003 논문 17-1-12

유한요소법에 의한 IH-Cooker의 열해석에 관한 연구

(A Study on the Thermal Analysis of Induction Heating Cooker with Finite Element Method)

오홍석*

(Hong - Seok Oh)

요 약

본 논문에서는 유도가열조리기의 효과적인 설계를 위하여 입력주파수 변화에 따른 유도가열조리기의 자계와 열계 해석 방법을 제시하였다. 유도가열조리기의 내부자계는 3차원 축대칭 유한요소법을 사용하여 해석하였으며, 열원은 유도가열조리기의 내부에서 유도된 와전류에 의하여 발생되고, 열은 열원과 열방정식을 사용하여 계산되어진다. 또한, 유도가열조리기의 온도특성을 스테인레스와 알루미늄 각각에 대하여 주파수와 투자율에 따라 제시하였다.

Abstract

Recently, induction heating cooker(IH-Cooker) is very interested for high efficiency, the quickness of heating time and the convenient regulation of heating spot. In this paper, we proposed the magneto-thermal analysis of an induction heating cooker(IH-Cooker) as an efficient design, and analyzed the magnetic field intensity inside the axisymmetric shaped cooker using three-dimensional axisymmetric finite element method(Flux2D) and the effectual heat source was obtained by ohmic losses from eddy currents induced in the cooker. Also, we presented the temperature characteristics of the IH-Cooker according to input frequency and relative permeability in stainless parts and in aluminum parts.

Key Words : Induction heating, FEM, IH-Cooker, Eddy current, Input frequency.

1. Introduction

Induction heating processes for heating provide significant technological, economic and ecological advantages in comparison with conventional oil or gas-fired furnace : fast heating rate, instant controllability, high efficient and minimal environment pollution[1]-[3]. Therefore induction heating is widely used in today's industry, in operations such as metal hardening, preheating for forging operations, or cooking. It is a complex process involving both electromagnetic and thermal phenomena. Recently, induction heating cooker

* 주저자 : 삼척대학교 소방방재학부 겸임교수
Tel : 033-570-6119, Fax : 033-535-0594
E-mail : ohhong@dreamwiz.com
접수일자 : 2002년10월18일
1차심사 : 2002년10월28일
심사완료 : 2003년12월 3일

(IH-Cooker) is very interested for high efficiency, the quickness of heating time and the convenient regulation of heating spot. The magnetic field intensity and the heat source in the IH-Cooker should be exactly calculated in order to make temperature distribution required on the surface of the IH-Cooker. But, the waste of time and cost has been increased because the design method of the IH-Cooker in the industry is depending on the experience. Therefore, it is continuously required that the development of precision design method is based on the exact magnetic field intensity and heat source. And, numerical simulation of IH-Cooker clearly involves two coupled phenomena : electromagnetism and heating. An efficient eddy current computation has to be performed in order to obtain the source term to be plugged into the heat equation[4]-[7].

In this paper, the magneto-thermal analysis of the IH-Cooker was presented as an efficient design. The magnetic field intensity inside the axisymmetric shaped cooker was analyzed using three-dimensional axisymmetric finite element method(FEM) and the effectual heat source was obtained by ohmic losses from eddy currents induced in the IH-Cooker. The heat was calculated using the heat source and heating equation. Also, it was represented the temperature characteristics of the IH-Cooker according to input frequency and relative permeability in stainless parts and in aluminum parts.

2. Three-dimensional Axisymmetric FEM

The construction of the IH-Cooker can apply to the three-dimensional axisymmetric FEM because it is the same form for circular direction. We can summarize the Maxwell's equation describing the systems with eddy currents as follows equation (1)~(5).

$$\nabla \times H = J \tag{1}$$

$$J = \sigma E \tag{2}$$

$$E = -\frac{\partial A}{\partial t} - \nabla \phi \tag{3}$$

$$B = \nabla \times A \tag{4}$$

$$B = \mu H \tag{5}$$

where H is the intensity of magnetic field, J is the sinusoidal exciting current density, σ is the electric conductivity of mass, E is the intensity of electric field, A is the magnetic vector potential, ϕ is the scalar potential, B is the magnetic flux density and μ is the permeability of mass. For the system, we can set the $\nabla \phi$ in equation(3) to zero[7], the final governing equation for A is the equation(6).

$$\frac{1}{\mu} \nabla^2 A = j\omega\sigma A - J \tag{6}$$

where ω represents the angular input frequency of the sinusoidal exciting current. The energy functional whose Euler-Lagrange equation is the same as governing equation(6) can be expressed as equation(7).

$$F = \int_S \frac{1}{2\mu} \left\{ \left(\frac{1}{r}\frac{\partial rA}{\partial z}\right)^2 + \left(\frac{1}{r}\frac{\partial rA}{\partial r}\right)^2 \right\} 2\pi r dr dz + \frac{j\omega}{2} \int_S \sigma A^2 \, 2\pi r dr dz - \int_S JA \, 2\pi r dr dz \tag{7}$$

After discretizing of the system, minimization condition of the energy functional equation(7) gives the system matrix equations(8).

$$[P]\{A\} + [Q]\{A\} = \{R\} \tag{8}$$

where [P] and [Q] are the coefficient matrices and {R} is the forcing vector. The coefficient matrices and the forcing vector can be assembled with element matrices written as equation(9)~(11).

$$[P]^e = \frac{1}{4\mu^e \triangle^e} \begin{bmatrix} b_l^2 + c_l^2 & b_l b_m + c_l c_m & b_l b_n + c_l c_n \\ b_l b_m + c_l c_m & b_m^2 + c_m^2 & b_m b_n + c_m c_n \\ b_l b_n + c_l c_n & b_m b_n + c_m c_n & b_n^2 + c_n^2 \end{bmatrix} \tag{9}$$

$$[Q]^e = \frac{j\omega\sigma^e \triangle^e}{12}\begin{bmatrix} 2 & 1 & 1 \\ 1 & 2 & 1 \\ 1 & 1 & 2 \end{bmatrix} \quad (10)$$

$$[R]^e = \frac{J^e \triangle^e}{3}\begin{bmatrix} 1 \\ 1 \\ 1 \end{bmatrix} \quad (11)$$

where $\triangle^e$ is the area of that element.

It can be calculated the magnetic vector potential, the eddy current and the heat source in each node by solving the system matrix equation. And the eddy current, J_e , is the equation(12) from ohms law as shown below.

$$J_e = \sigma E_e = -\sigma\frac{\partial A}{\partial t} = -j\omega\sigma A \quad (12)$$

The heat source per unit volume, $h_{ts}[\,W/m^3\,]$, is written as equation(13).

$$h_{ts} = \frac{|J_e|^2}{\sigma} = \omega^2\sigma|A|^2 = \omega^2\sigma AA^* \quad (13)$$

3. Magnetic Analysis

Table 1 and Fig. 1 are respectively the material constants and scales of the IH-Cooker and the actual shape for the exciting coil of it.

Table 1. The material constants and the scales of the IH-Cooker

	Stainless Steel	Aluminum
Relative permeability (μ_r)	1(case 1) 10(case 2)	0.25×10^{-7}
Electric conductivity (σ)	1.667×10^6	4.0×10^7
Thermal conductivity (k)	30	204
Thickness [mm]	$0.8^{\pm0.05}$	$3.0^{\pm0.15}$
Radius of bottom [mm]	115.2	111.4
Height [mm]	83.94	83.94

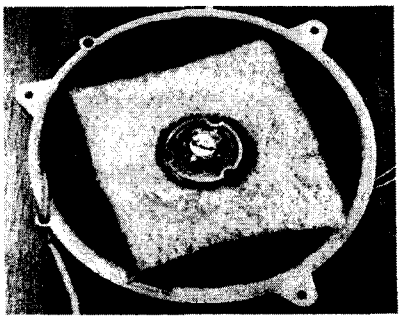

Fig. 1. Exciting coil

Fig. 2 is the three-dimensional axisymmetric FE-model of the IH-Cooker, and is the structure of double layer with aluminum and stainless. Fig. 3 is the flux lines of case 1($\mu_r = 1$) with the leakage flux at the inner IH-Cooker and Fig. 4 is the flux lines of case 2($\mu_r = 10$). Here we know that the flux lines cannot pass through the inner IH-Cooker because of the skin effect of the stainless steel.

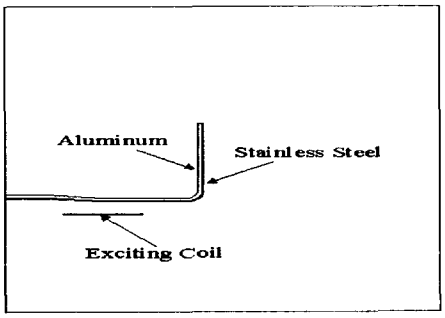

Fig. 2. The FE-model of the IH-Cooker

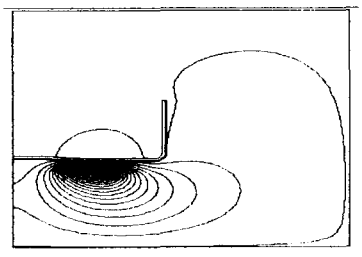

(Input frequency=25[kHz], $\mu_r = 1$)

Fig. 3. The flux lines of the IH-Cooker

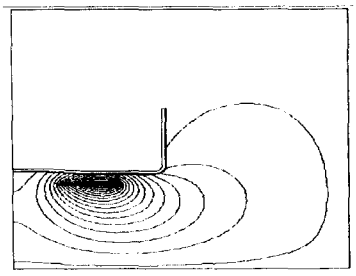

(Input frequency=25[kHz], $\mu_r = 10$)
Fig. 4. The flux lines of the IH-Cooker

4. Thermal Analysis

The three-dimensional axisymmetric heat conduction equation in the steady state is expressed as follow:

$$\frac{1}{r}\frac{\partial}{\partial r}(kr\frac{\partial T}{\partial r})+\frac{\partial}{\partial z}(k\frac{\partial T}{\partial z}) = -h_{ts} \quad (14)$$

where h_{ts} is the heat sources and k is the thermal conductivity. The complex boundary condition between the surface of the IH-Cooker and the area around it is described by equation (15).

$$-k\frac{\partial T}{\partial n} = h(T-T_\infty) \quad (15)$$

where h is the convective exchange coefficient, T is the temperature in the boundary surfaces, T_∞ is the temperature of the fluid and $\frac{\partial T}{\partial n}$ is the normal component of the temperature in boundary surfaces. Arranging equation (14), we obtain equation (16).

$$-\frac{\partial}{\partial r}(r\frac{\partial T}{\partial r})-\frac{\partial}{\partial z}(r\frac{\partial T}{\partial z}) = r\frac{h_{ts}}{k} \quad (16)$$

The heat conduction equation can be obtained with the standard Galerkin's method as follows.

$$\int\int_A\left\{r(\frac{\partial T}{\partial r})^2 + r(\frac{\partial T}{\partial z})^2\right\}2\pi r dr dz$$

$$= \int\int_A 2Tr(\frac{h_{ts}}{k})2\pi r dr dz \quad (17)$$

And the element matrix can be expressed by the equations (18), (19) and (20).

$$K^e T^e = f^e \quad (18)$$

$$K_{ij}^e = \frac{\pi}{2\Delta^e} r_0{}^2(c_i c_j + d_i d_j) \quad (19)$$

$$f_i^e = \frac{\pi r_0 \Delta^e}{6}\frac{h_{ts}}{k}(2r_i + r_j + r_k) \quad (20)$$

where r_0 is $(r_1 + r_2 + r_3)/3$.

Also, the element matrix equation in the complex boundary is expressed as follows:

$$[K^e + \overline{K^e}]T^e = [f^e + \overline{f^e}] \quad (21)$$

where,

$$\overline{K^e} = \int_{A_2^e}\sigma N^{et} N^e dS \quad (22)$$

$$\overline{f^e} = \int_{A_2^e} g N^{et} dS \quad (23)$$

where σ is h/k, g is hT_∞/k and A_2^e is the elements on the boundary with the complex boundary condition.

If σ is constant inside an element and the opposite side of node $i-th$ is the complex boundary surface, the equations (22) and (23) can be respectively expressed in terms of equations (24) and (25).

$$[\overline{K^e}]_i = \frac{\pi\sigma(c_i{}^2 + d_i{}^2)^{1/2}}{6} \times \begin{bmatrix} 3r_k + r_j & 0 & r_k + r_j \\ 0 & 0 & 0 \\ r_k + r_j & 0 & r_k + 3r_j \end{bmatrix} \quad (24)$$

$$[\overline{f^e}]_i = \frac{\pi g(c_i{}^2 + d_i{}^2)^{1/2}}{3}\begin{bmatrix} 2r_k + r_j \\ 0 \\ r_k + 2r_j \end{bmatrix} \quad (25)$$

Substituting equation (21) into equations (24) and (25), we can obtain the element matrix with the complex boundary condition. The system matrix is constructed using the above equations and is solved using the ICCG(Incomplete Choleski Conjugate Gradient) algorithm, and the temperatures in each node can be obtained.

5. Temperature Characteristics

Fig. 5 represents points to calculate the temperature in stainless steel parts and in aluminum parts. Figs. 6 and 7 represent respectively the temperature characteristics of the IH-Cooker according to input frequency and relative permeability in stainless steel parts and in aluminum parts.

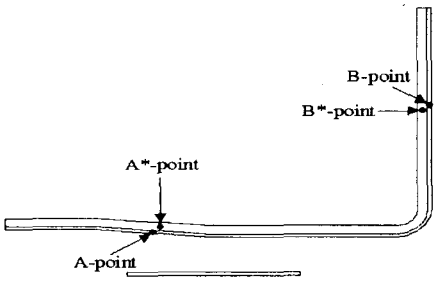

Fig. 5. Points to calculate the temperature

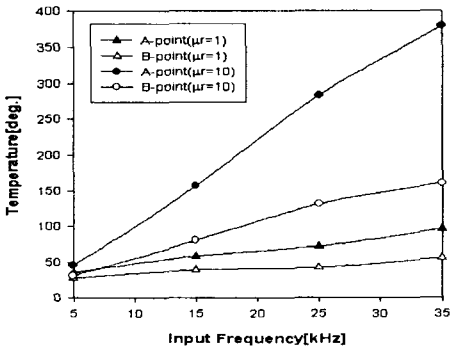

Fig. 6. The temperature curve of the IH-Cooker in stainless steel.

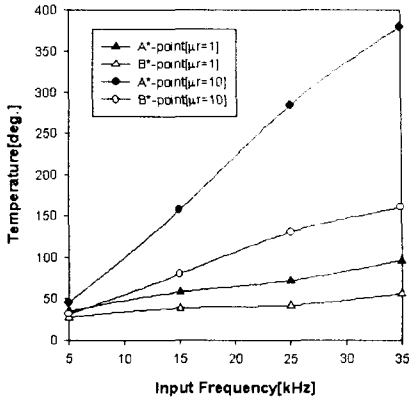

Fig. 7. The temperature curve of the IH-Cooker in aluminum.

We know that the temperature of aluminum is higher than that of stainless steel at point distant from the heat source because the thermal conductivity of aluminum is larger than that of stainless steel. Also we know that the temperature of the IH-Cooker is rapidly reached its peak value as the value of relative permeability and of input frequency are high.

6. Conclusions

In this paper, the magneto-thermal of IH-Cooker was analyzed using three- dimensional axisymmetric finite element method(FEM). And the heat was calculated using the heat source and heating equation. Also, it was represented the temperature characteristics of the IH-Cooker according to input frequency and relative permeability in stainless parts and in aluminum parts. The temperature of aluminum is higher than that of stainless steel at point distant from the heat source because the thermal conductivity of aluminum is larger than that of stainless steel. Also we know that the temperature of the IH-Cooker is rapidly reached its peak value as the value of relative permeability and of frequency are high.

References

[1] Zanming Wang, Xiaoguang Yang, Youhua Wang and Weili Yan, "Eddy Current and Temperature Field Computation in Transverse Flux Induction Heating Equipment for Galvanizing Line", IEEE Trans. on Mag., Vol.37, No.5, pp.3437-3439, 2001.

[2] Piotr Urbanek, Adam Skork, "Magnetic Flux and Temperature Analysis in Induction Heated Steel Cylinder", IEEE Trans. on Mag., Vol.30, No.5, pp.3328-3330, 1994.

[3] Yoshihiro Kawase, Tsutomu Miyatake, Katsuhiro Hirata, "Thermal Analysis of Steel Blade Quenching by Induction Heating", IEEE Trans. on Mag., Vol.36, No.4, pp.1788-1791, 2000.

[4] Masato Enokizono, Takashi Todaka, Shotaro Nishimura, "Finite Element Analysis of High-Frequency Induction Heating Problems Considering Inhomogeneous Flow of Exciting Currents", IEEE Trans. on Mag., Vol.35, No.3, pp.1646-1649, 1999.

[5] C. Chaboudez, S. Clain, R. Glardon, etc., "Numerical Modeling in Induction Heating for Axisymmetric Geometries", IEEE Trans. on Mag., Vol.33, No.1, pp.739-745, 1997.

[6] Zs. Badics, H. Riedler, H. Stogner, "Application of FEM to Coupled Electric, Thermal and Mechanical Problems", IEEE Trans. on Mag., Vol.30, No.5, pp.3316-3319, 1994.

[7] Tanroku Miyoshi, Munehiko Sumiya, Hideki Omori, "Analysis of an Induction Heating System by Finite Element Method", T.IEE Japan, RM-86-53, PP.117-125, 1986.

[8] Tatsuya FURUKAWA, Itsuya MUTA and Tatsuhiko KOSUGI, "Finite Element Analysis of Induction Heating Range", Reports of the Faculty of Science and Engineering, Saga University, PP. 81-87, 1988.

[9] Hong-Seok Oh, etc., "A Study on the Heat-Diffused Prediction of Induction Heating Jar using Finite Element Method", International conference IEB, pp.234-240, 2002.

◇저자소개◇

오 홍 석(吳鴻錫)

1969년 1월 9일생. 1992년 영남대 공대 전기공학과 졸업(학사). 1994년 영남대 공대 전기공학과 졸업(석사). 2000년 동 대학원 전기공학과 졸업(박사). 현재 삼척대 제2공학부 소방방재학부 겸임교수. (주)이맥스하이테크 대표이사.

e-mail : ohhong@dreamwiz.com